0021-972X/07/$15.00/0
Printed in U.S.A.

The Journal of Clinical Endocrinology & Metabolism 92(4):1458–1466

doi: 10.1210/jc.2006-2199

RbAp48 is a Target of Nuclear Factor-κB Activity in Thyroid Cancer

Francesco Pacifico, Michele Paolillo, Gennaro Chiappetta, Elvira Crescenzi, Simona Arena, Andrea Scaloni, Mario Monaco, Carlo Vascotto, Gianluca Tell, Silvestro Formisano, and Antonio Leonardi

Istituto di Endocrinologia e Oncologia Sperimentale (F.P., E.C.), Consiglio Nazionale delle Ricerche, 80131 Naples, Italy; Dipartimento di Biologia e Patologia Cellulare e Molecolare (M.P., S.F., A.L.), "Federico II" University of Naples, 80131 Naples, Italy; Functional Genomic Unit (G.C., M.M.), Istituto Nationale Tumori Fondazione G. Pascale, 80131 Naples, Italy; Laboratorio di Proteomica e Spettrometria di Massa (S.A., A.S.), Istituto per il Sistema di Produzione Animale in Ambiente Mediterraneo, Consiglio Nazionale delle Ricerche, 80147 Naples, Italy; and Dipartimento di Scienze e Tecnologie Biomediche (C.V., G.T.), University of Udine, 33100 Udine, Italy

Context: We have recently shown that nuclear factor (NF)-κB activity is constitutively elevated in anaplastic human thyroid carcinomas. The inhibition of NF-κB in the anaplastic thyroid carcinoma cell line (FRO) leads to increased susceptibility to apoptosis induced by chemotherapeutic drugs and to the block of oncogenic activity.

Objectives: To understand better the molecular mechanisms played by NF-κB in thyroid oncogenesis, we performed a differential proteomic analysis between FRO transfected with a superrepressor form of inhibitor of κBα (IκBαM) and the parental counterpart (FRO Neo cells).

Results: Differential proteomic analysis revealed that the retinoblastoma-associated protein 48 (RbAp48) is down-regulated in the absence of functional NF-κB. Immunohistochemical analysis of normal and pathological human thyroid specimens confirmed that RbAp48 is strongly overexpressed in primary human carcinomas. Reduction of RbAp48 expression using small interfering RNA determined the suppression of tumorigenicity, very likely due to the decrease of their growth rate rather than to an increased susceptibility to apoptosis. In addition, we showed that NF-κB, at least in part, transcriptionally controls RbAp 48. A functional NF-κB consensus sequence was located within the promoter region of RbAp48 human gene, and embryonic fibroblasts isolated from the p65 knockout mouse (murine embryonic fibroblasts $p65^{-/-}$) showed decreased expression of RbAp48.

Conclusion: Our results show that RbAp48 is a NF-κB-regulated gene playing an important role in thyroid cancer cell autonomous proliferation. **(*J Clin Endocrinol Metab* 92: 1458–1466, 2007)**

NUCLEAR FACTOR (NF)-κB is a family of transcription factors regulating the expression of several genes controlling apoptosis, inflammation, immune response, and cancer (1). NF-κB is usually present as a p65-p50 heterodimer in a latent form in the cytoplasm, bound to the inhibitors of κB (IκBs) inhibitory proteins (2). A wide spectrum of extracellular signals (proinflammatory cytokines, bacterial and viral infections, oxidative stress, *etc.*) gives rise to a signaling cascade converging on the IκB kinase (IKK) complex, responsible for phosphorylation of IκB proteins and their subsequent degradation through a proteasome-dependent pathway (3,4). Degradation of IκB liberates the p65-p50 heterodimer to enter the nucleus and activate transcription of target genes. These targets are in four major categories: 1) genes controlling inflammation and immunity, 2) antiapoptotic genes, 3) genes that positively regulate cell proliferation, and 4) genes that negatively regulate NF-κB (5).

Because the development of a malignant tumor requires several changes in cellular metabolism, it is not surprising that the NF-κB pathway, which influences different aspects of cell physiology, may be involved in cell transformation. Several studies show that the inhibition of constitutive NF-κB activity blocks the oncogenic potential of neoplastic cells in different ways: 1) sensitizing tumor cells to chemotherapeutic drug-induced apoptosis, 2) decreasing the highly proliferative rate that characterizes transformed cells, and 3) inhibiting tissue invasiveness and metastatic potential of highly malignant cells (6). In addition, because it is now generally accepted that chronic inflammation contributes to the genesis of many solid tumors, such as gastric, colon, or hepatic carcinomas, it has been recently shown that activation of NF-κB by the classical IKKβ-dependent pathway is a crucial mediator of inflammation-induced tumor growth and progression in animal models of inflammation-associated cancer (7, 8). The inhibition of NF-κB activity has been effective in blocking neoplastic transformation either *in vitro* or *in vivo* experimental models, and, therefore, in recent years several NF-κB pharmacological inhibitors have been developed to interfere with NF-κB activity in cancer (9, 10). These inhibitors have been shown to have efficacy in blocking tumorigenicity in different types of cancer cells, but their use as potential drugs is still away from clinical use because they also block the physiological functions of NF-κB, such as the control of inflammatory and immune responses. Therefore, a great effort has been made to identify NF-κB-controlled

First Published Online January 23, 2007

Abbreviations: 2-DE, 2-Dimensional gel electrophoresis; HDAC, histone deacetylase; IκB, inhibitor of κB; IKK, IκB kinase; MALDI-TOF-MS, matrix-assisted laser desorption ionization-time of flight-mass spectrometry; MEF, murine embryonic fibroblasts; NF, nuclear factor; SDS, sodium dodecyl sulfate; siRNA, small interfering RNA.

JCEM is published monthly by The Endocrine Society (http://www.endo-society.org), the foremost professional society serving the endocrine community.

genes that mediate some of the NF-κB functions, to block selectively some but not all of the NF-κB activities.

RbAp48, a 48-kDa protein initially characterized for its ability to bind to the retinoblastoma protein Rb (11), is a member of several chromatin-remodeling complexes, such as the nucleosome remodeling histone deacetylase (HDAC) complex (12), the Sin3 complex, which contains HDACs (13), and the CAF-1 complex, a chromatin assembly factor coupled to DNA synthesis (14). It has been hypothesized that RbAp48 connects the histones with the subunits of these complexes (14) and that it is required for transcriptional repression mediated by HDACs (15). In particular, it has been shown that RbAp48 belongs to the HDAC complex associated to Rb (16, 17) and that its *Drosophila* ortholog p55 is required for the repression of dE2F2/RBF-regulated genes (18). Very little is known about the role of RbAp48 in cancer, and no evidence is about the involvement of NF-κB in the regulation of RbAp48 expression. Here, by using a differential proteomic approach, we detected a reduced expression of RbAp48 in cells lacking functional NF-κB and investigated its role in thyroid tumorigenesis.

Materials and Methods

Cell culture and biological reagents

FRO (19), FRO IκBαM (20), FRO RbAp48 small interfering RNA (siRNA), HEK293, murine embryonic fibroblasts (MEFs), and MEFs $p65^{-/-}$ (21) cell lines were grown in DMEM (Sigma, St. Louis, MO) supplemented with 10% fetal bovine serum (Sigma). Anti-RbAp48 (PC-546) and anti-actin (sc-8432) antibodies were purchased from Oncogene Research Products (San Diego, CA) and Santa Cruz Biotechnology, Inc. (Santa Cruz, CA), respectively. Human TNF-α was from Peprotech (Rocky Hill, NJ).

Preparation of nuclear extracts and 2-dimensional gel electrophoresis (2-DE) analysis

Cell nuclear extracts were prepared as previously described (22, 23). The 2-DE analysis was performed in triplicate on nuclear extracts from three different batches of cell cultures. A total of 30–50 μg of nuclear cell extracts were loaded onto 13 cm, pH 3–10, 4–7, or 6–11 L-IPG strips (Amersham-Pharmacia Biosciences, Milan, Italy). Isoelectric focusing was performed using an IPGPhor II system (Amersham-Pharmacia Biosciences) according to the manufacturer's instructions. Focused strips were equilibrated with 6.0 M urea, 26 mM dithiothreitol, 4% (weight/vol) sodium dodecyl sulfate (SDS), 30% (vol/vol) glycerol in 0.1 M Tris-HCl (pH 6.8) for 15 min, followed by 6.0 M urea, 0.38 M iodoacetamide, 4% (weight/vol) SDS, 30% (vol/vol) glycerol, and a dash of bromophenol blue in 0.1 M Tris-HCl (pH 6.8), for 10 min. The equilibrated strips were applied directly to SDS-10% (weight/vol) polyacrylamide gels and separated at 130 V. Gels were fixed and stained by ammoniacal silver (24). Gels were scanned with an Image Master 2-D apparatus and analyzed by the Melanie 5 software (Amersham-Pharmacia Biosciences) that allowed estimating relative differences in spot intensities for each represented protein. Statistical analysis of differentially expressed proteins was performed as previously described (25) on about 200 different matched spots in the different pH ranges from each sample.

Mass spectrometry analysis

Spots from 2-DE were excised from the gel, triturated, and washed with water. Proteins were in-gel reduced, S-alkylated, and digested with trypsin as previously reported (25). Digest aliquots were removed and subjected to a desalting/concentration step on μZipTipC_{18} (Millipore, Bedford, MA) using acetonitrile as eluent before matrix-assisted laser desorption ionization-time of flight-mass spectrometry (MALDI-TOF-MS) analysis. Peptide mixtures were loaded on the MALDI target, using the dried droplet technique and α-cyano-4-hydroxycinnamic acid as matrix, and analyzed using Voyager-DE PRO mass spectrometer (Applied Biosystems, Framingham, MA). Internal mass calibration was performed with peptides deriving from trypsin autoproteolysis. The PROWL software package was used to identify spots unambiguously (estimated Z score more than two) from independent nonredundant sequence databases (26). Candidates from peptide matching analysis were further evaluated by the comparison with their calculated mass and pI using the experimental values obtained from 2-DE.

Immunohistochemical analysis

Specimens from normal and pathological human thyroid were isolated, rinsed with PBS, fixed in 4% buffered neutral formalin, and embedded in paraffin. Then, 5–6-μm thick paraffin sections were deparaffinized and placed in a solution of absolute methanol and 0.3% hydrogen peroxide for 30 min, then washed in PBS before immunoperoxidase staining. Slides were then incubated in a humidified chamber with antibody anti-RbAp48 diluted 1:100 in PBS, overnight at 4 C and subsequently incubated, first with biotinylated goat antirabbit IgG for 20 min (VECTASTAIN ABC Systems; Vector Laboratories, Burlingame, CA), and then with premixed reagent ABC (Vector Laboratories) for 20 min. The immunostaining was performed with rabbit polyclonal anti-RbAp48 antibody by incubating slides in diaminobenzidine (DakoCytomation, Fort Collins, CO) solution containing 0.06 mM diaminobenzidine and 2 mM hydrogen peroxide in 0.05% PBS pH 7.6 for 5 min, and after chromogen development, slides were washed, dehydrated with alcohol and xylene, and mounted with coverslips using a permanent mounting medium (Permount; Biomeda, Burlingame, CA). Two investigators independently scored the slides. Informed consent was obtained from the patients, and the institutional review board committee approved the study.

siRNA of RbAp48

To knock-down RbAp48 expression, we designed double-stranded oligonucleotides containing sequences derived from the human RbAp48 ORF (nucleotides 849–867 and 1197–1215) in forward and reverse orientation separated by a 7-bp spacer region (caagaga) to allow the formation of the hairpin structure in the expressed siRNAs. RbAp48 siRNA 849: sense strand, 5′ – aattcGGATACTCGTTCAAACAATcaagagaATTGTTTGAACGAGTATCCttttttc; antisense strand, 5′ – tcgagaaaaaGGATACTCGTTCAAACAATtctcttgATTGTTTGAACGAGTATCCg. RbAp48 siRNA 1197: sense strand, 5′ – aattcTGGTCATACTGCCAAGATAcaagagaTATCTTGGCAGTATGACCAttttttc; antisense strand, 5′ – tcgagaaaaaTGGTCATACTGCCAAGATAtctcttgTATCTTGGCAGTATGACCAg. (*Lowercase letters* at the 5′ and 3′ ends of the oligos indicate restriction sites. *Lowercase letters* in the middle of the sequence indicate the hairpin sequence.) The resulting double-stranded oligonucleotides were cloned into the pcRNAi vector that we derived from the pcDNA3.1 vector (Invitrogen, Carlsbad, CA) by replacing the viral promoter-cassette with the H1 promoter that is specifically recognized by RNA polymerase III (27).

Northern and Western blots

For Northern blot, 20 μg of total RNA from parental and transfected FRO cell lines as well as from MEFs and MEFs $p65^{-/-}$ were analyzed by electrophoresis on a 1.2% formaldehyde agarose gel and blotted onto nitrocellulose membrane (Bio-Rad, Hercules, CA), as described (28). For Western blot, 50 μg of total proteins from cell lysates were analyzed by 10% SDS-PAGE and blotted onto polyvinylidene difluoride sheets (Millipore). Filters were blocked for 1 h at room temperature with 10% nonfat dry milk in Tris-buffered saline with Tween 20 buffer and incubated with 1:2000 dilution of anti-RbAp48 or anti-actin antibodies, overnight at 4 C.

In vitro tumorigenicity assays

To analyze the ability of the various FRO clones to form colonies in soft agar, 1×10^4 cells were seeded in 60-mm dishes onto 0.3% Noble Agar (Difco, Detroit, MI) on top of a 0.6% bottom layer. Colonies larger than 50 cells were scored after 2 wk incubation at 37 C (29).

Cytotoxic treatments and measurements of apoptosis

There were 2.5×10^5 cells/well seeded in six-well culture plates and incubated for 24 and 48 h at 37 C with different concentrations of cisplatin or doxorubicin. Cell death was assessed by measuring caspase activity by the CaspACE FITC-VAD-FMK In Situ Marker (Promega, Madison, WI), a fluoroisothiocyanate conjugate of the cell permeable inhibitor VAD-FMK, according to the manufacturer's instructions. Samples were analyzed by flow cytometry using a CyAn ADP (DakoCytomation), equipped with Summit V4.2 Software. Results were mean ± SD of at least three separate experiments.

[^{3}H]-thymidine DNA incorporation

There were 5×10^4 cells/well seeded in 12-well culture plates and incubated for 4 h at 37 C with 0.5 μCi/well of [^{3}H]-thymidine (Amersham-Pharmacia Biosciences). After three washings with cold PBS, cells were incubated for 10 min at 4 C with 0.5 ml of 20% trichloroacetic acid. The trichloroacetic acid was then removed, and cells were lysed with gentle shaking for 30 min at 37 C in the presence of 1 N NaOH (0.5 ml/well). An aliquot of lysates (0.1 ml) was used to evaluate the protein content by colorimetric assay (Bio-Rad), while the remnant was analyzed at the β-counter (Beckman Coulter, Inc., Fullerton, CA) after adding an equal volume (0.4 ml) of HCl 1 N to neutralize the samples. Results were the mean ± SD of two separate experiments. Results were normalized on total protein content.

Analysis of the NF-κB consensus sequence in the RbAp48 promoter region

A 2.0-kb *Nhe*I-*Xho*I genomic fragment PCR-amplified, containing the 5′-flanking region of the human *RbAp48* gene, was subcloned between the corresponding restriction sites of the luciferase expression vector pGL3 Basic (Promega). The Quickchange Site-Directed Mutagenesis Kit (Stratagene, La Jolla, CA) used the resulting plasmid, p2.0RbAp48 WT, as a template for PCR generation of the mutant p2.0RbAp48 Mut plasmid. The p2.0RbAp48 Mut plasmid contained three point mutations in the κB-site located in the promoter region of *RbAp48* gene (see Fig. 2B). The activity of the three plasmids was evaluated in HEK293 cells, stimulated with human TNFα (2000 U/ml) for 3 h, or left untreated. Cell extracts were prepared, and reporter gene activity was determined via the luciferase assay system (Promega). Expression of the β-gal vector (0.2 μg) was used to normalize transfection efficiencies.

Statistics

Data were analyzed using ANOVA test analysis. Data are presented as the means ± SD. P values < 0.05 were considered significant.

Results

Differences in proteome profile between FRO Neo and FRO IκBαM cell lines

To identify molecular processes associated with the loss of NF-κB transcriptional activity, we have chosen an unbiased strategy by studying the differences in the nuclear proteome profile between the anaplastic thyroid cell line FRO Neo and a cell line stably transfected with a super-repressor form of IκBα (FRO IκBαM) (20). A differential proteomic approach based on 2-DE gel quantitative analysis coupled to MALDI-TOF-MS identification of the up-regulated/down-regulated proteins has been used. In addition to proteins up-regulated/down-regulated, this approach allows detection also of qualitative difference between the two samples. To maximize possible differences at the proteome level, nuclear samples have been analyzed in three different pH ranges (*i.e.* pH 3–10, 4–7, and 6–11) (data not shown). Silver staining of 2-DE has allowed for the visualization, and simultaneous quantitative and qualitative evaluation of about 200–250 protein spots in each gel. For each pH gradient, a different number of matching spots have been obtained, and a total of 19 proteins showed statistically significant quantitative or qualitative differences, when comparing proteomic maps of nuclear samples of the two different cell lines (data not shown). MALDI-TOF peptide mass fingerprint analysis successfully identified six spots (see supplemental Table 1, published as supplemental data on The Endocrine Society's Journals Online web site at http://jcem.endojournals.org).

Of proteins whose expression was down-regulated in FRO IκBαM cells, RbAp48 showed a marked decrease (Fig. 1A). We confirmed this result using both Northern and Western blot. RbAp48 expression was decreased in FRO IκBαM clones compared with FRO Neo cells (Fig. 1, B and C).

RbAp48 is a gene under NF-κB transcriptional control

To address deeply the role of NF-κB in controlling transcription of RbAp48, we analyzed its expression in mouse embryonic fibroblasts derived from the p65 knockout mouse (MEFs p65$^{-/-}$). Both Northern and Western blot assays evidenced a decreased expression of RbAp48 in MEFs p65$^{-/-}$

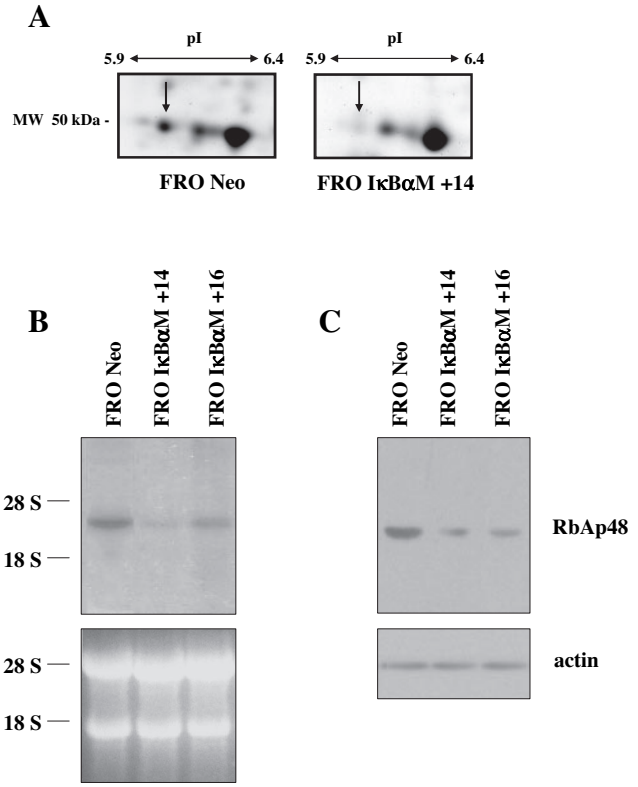

FIG. 1. Analysis of RbAp48 expression in FRO Neo and FRO IκBαM cell lines. The differential proteomic approach, based on 2-DE gel quantitative analysis coupled to MALDI-TOF-MS identification, revealed that RbAp48 expression was down-regulated in FRO IκBαM +14 cells compared with the parental counterpart FRO Neo (A, *arrows*). Northern (B, *top*) and Western (C, *top*) blots confirmed the different levels of RbAp48 expression between FRO Neo and FRO IκBαM cell lines. The expression of RbAp48 mRNA was normalized on total RNA content (B, *bottom*), that of RbAp48 protein on actin expression levels (C, *bottom*).

compared with wild-type MEFs (Fig. 2A). To investigate whether NF-κB was directly controlling RbAp48 expression, we isolated the RbAp48 gene promoter and analyzed the presence of canonical κB sites. The analysis performed by the MatInspector V2.2-TRANSFAC 4.0 database (Genomatix Software, Munich, Germany) revealed the presence of a potential NF-κB consensus sequence at about 1500 bp upstream the hypothetical transcription start site. Thus, a 2000 bp DNA fragment of RbAp48 human gene, containing the theoretical κB-site, transcription start site, and ATG translation start site, was cloned upstream to a promoterless luciferase reporter gene. In addition, we constructed two additional vectors, one in which the canonical κB site was mutated, and one lacking the κB site (Fig. 2B). The resulting plasmids were transfected in HEK293 cells, and both the basal and induced luciferase activity were measured. We did not detect any statistically significant difference in the basal activity of the three promoters (Fig. 2C). Instead, after treatment with TNF-α, a potent inducer of NF-κB, deletion of the κB site or its point mutation reduced the activity of the reporter plasmid by at least 50%. These data suggest that NF-κB is, at least in part, controlling the induced expression of RbAp48.

RbAp48 expression in human thyroid carcinomas

Because we previously found that primary human thyroid anaplastic carcinomas show highly constitutive NF-κB activity (20), we tested whether the RbAp48 expression paralleled the levels of NF-κB in human primary thyroid cancer. Human specimens from normal thyroid, papillary, follicular, and anaplastic thyroid carcinomas were collected and stained with anti-RbAp48 polyclonal antibodies (Fig. 3). The results of these experiments are summarized in Table 1. Low staining for RbAp48 was detected in normal thyroid follicular cells, while all tumor specimens showed a strong RbAp48 expression. In particular, RbAp48 staining increased with the malignant phenotype of thyroid carcinomas, reaching the highest levels of expression in anaplastic thyroid carcinomas (Table 1), in parallel to NF-κB activity (20). These results show

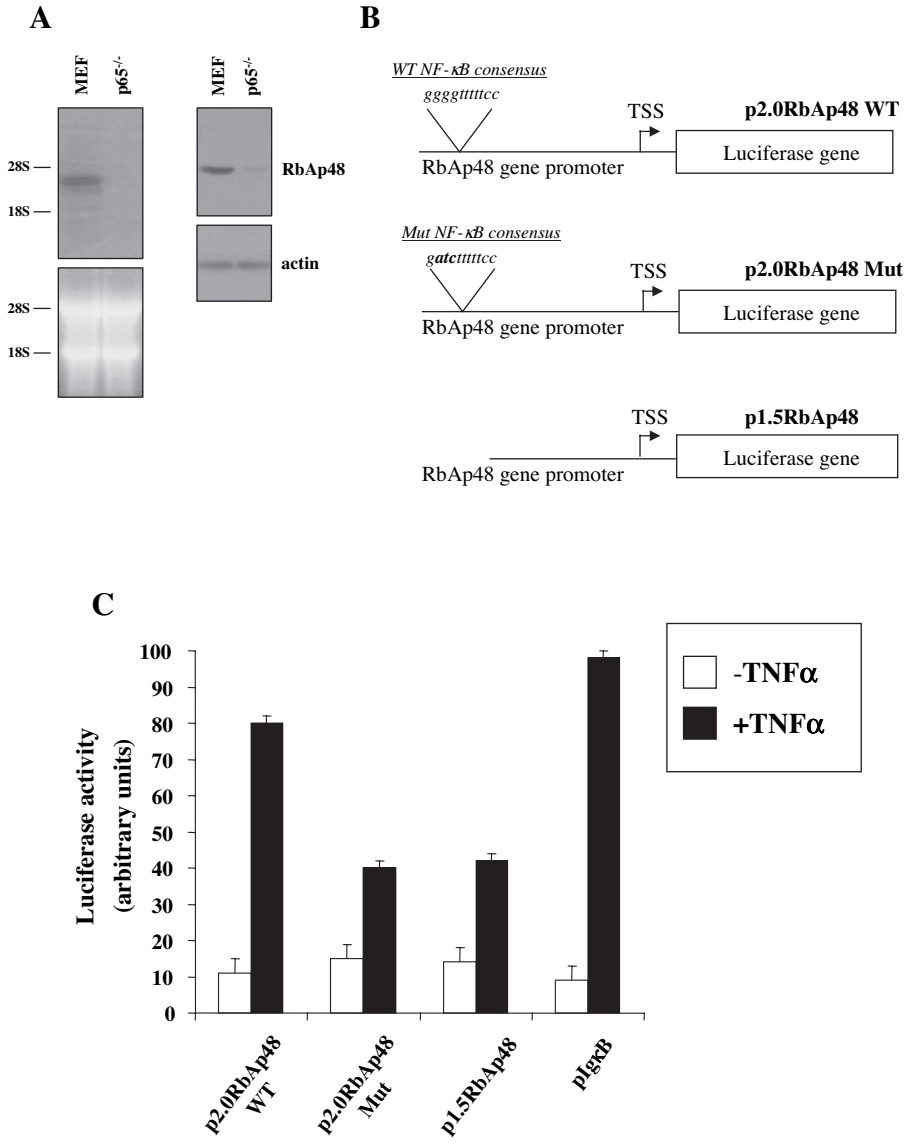

FIG. 2. NF-κB-dependent regulation of RbAp48 gene transcription. Northern (A, *left*) and Western (A, *right*) blot assays showed that RbAp48 is expressed at a lower level in $p65^{-/-}$ MEF compared with wild type (WT) MEF. Schematic representation of the plasmid generated to evaluate functionality of the κB site in the RbAp48 promoter (B). The mutated bases are indicated in *bold*. Basal and TNF-α-induced luciferase activity of the three constructs (C) illustrated in Fig. 2B. The result of a representative experiment performed is shown in triplicate, after normalization with β-galactosidase activities (mean ± SD). Similar results were obtained in three additional experiments.

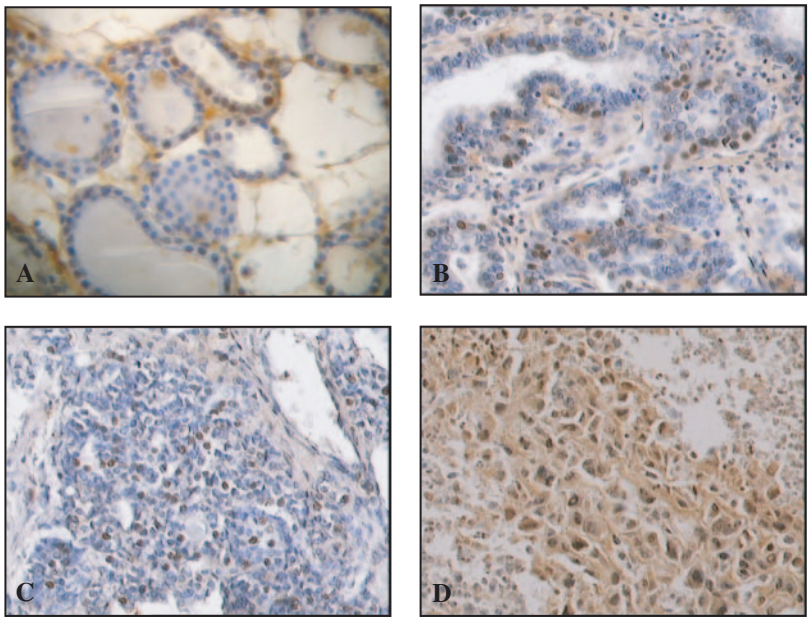

FIG. 3. Immunohistochemical analysis of RbAp48 expression in normal and pathological human thyroid tissues. Localization of RbAp48 *in situ* was determined by immunohistochemistry in sections from normal thyroid tissue (A), papillary thyroid carcinoma (B), follicular thyroid carcinoma (C), and anaplastic thyroid carcinoma (D). Magnification, ×400.

that RbAp48 is overexpressed in human thyroid tumors, supporting a role for this protein in thyroid cancer.

Role of RbAp48 in thyroid carcinomas

To analyze the role of RbAp48 in thyroid cancer, we decreased its expression in FRO cells by stable transfection of a siRNA plasmid designed for RbAp48 silencing. FRO RbAp48 siRNA clones were isolated after antibiotic selection and analyzed for the expression level of RbAp48. As shown in Fig. 4, both Northern (Fig. 4A) and Western (Fig. 4B) analysis revealed the silencing of RbAp48 expression in at least three of the various clones analyzed (indicated as 849 + 4, +21, and +29, respectively). Indeed, FRO cells transfected either with the empty vector (FRO Neo cells) or a control siRNA (indicated as 1197-3) still expressed RbAp48 mRNA and protein (Fig. 4).

Next, we investigated the tumorigenic potential of three clones (849 + 4, +21, and +29) by analyzing their ability to form colonies in soft agar. Although FRO Neo and the control clone 1197-3 were able to grow in agar, contributing to large and numerous foci of transformation (Fig. 5, *top*), 849 siRNA clones did not form any colony (Fig. 5, *bottom*).

To gain more insight into the mechanisms by which RbAp48 plays its role in thyroid carcinomas, we analyzed the susceptibility of parental FRO cells and 849 siRNA clones to chemotherapeutic drug-induced apoptosis, and their proliferative rate. Treatment of cells with increasing amounts of cisplatin (Fig. 6A) and doxorubicin (Fig. 6B) induced cell death at a similar extent in FRO cells and 849 siRNA clones, indicating that the sensitivity to drug-induced apoptosis did not change after inhibition of RbAp48 expression. Therefore, we investigated the autonomous proliferative rate of parental and transfected FRO cells by [^{3}H]-thymidine DNA incorporation in absence of serum. As shown in Fig. 7, 849 siRNA clones incorporated less [^{3}H]-thymidine (~50%) in their DNA than FRO Neo and 1197-3 cells, indicating that they grew more slowly than the parental FRO cells. Similar results were obtained by performing the experiment in the presence of serum (data not shown).

These results show that the decreased expression of RbAp48 by siRNA leads to the inhibition of the autonomous cell growth potential, suggesting that RbAp48 could influence the function of genes involved in the control of the cell cycle rather than apoptosis.

Discussion

One of the most exciting challenges in the study of NF-κB-mediated oncogenesis is the identification of NF-κB target genes mediating some of the NF-κB functions, specifically expressed (or overexpressed) in neoplastic cells. The

TABLE 1. Immunohistochemical analysis of RbAp48 expression in normal and pathological human thyroid tissues

Histological type of thyroid samples	No. of total cases analyzed by immunohistochemistry	No. of positive cases/no. of total cases analyzed by immunohistochemistry	RbAp48 staining score
Normal thyroid	2	2/2	1+
Papillary carcinoma	5	5/5	2+
Follicular carcinoma	3	3/3	3+
Anaplastic carcinoma	3	3/3	4+

Human specimens from normal thyroid, papillary, follicular, and anaplastic thyroid carcinomas were collected and stained with anti-RbAp48 polyclonal antibodies. The percentage of malignant cells stained was scored from 0–4: 0, negative cells; 1+, <10% of positive cells; 2+, 11–50% of positive cells; 3+, 51–75% of positive cells; and 4+, 76–100% of positive cells.

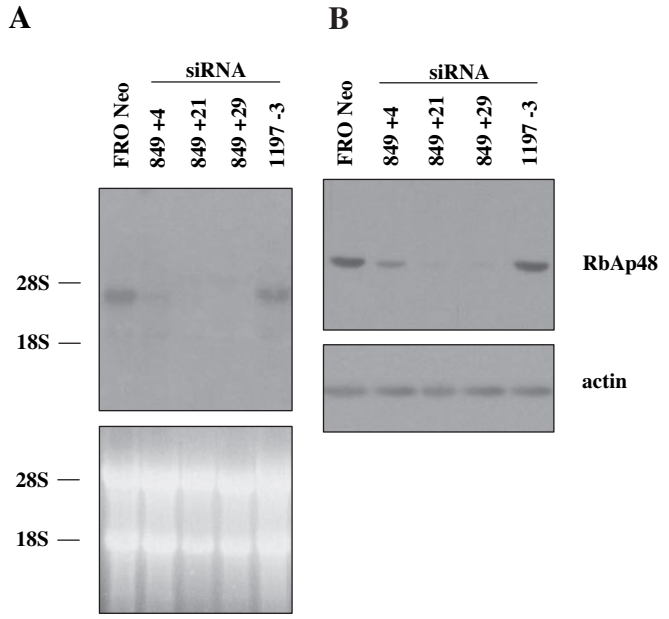

FIG. 4. Inhibition of RbAp48 expression by siRNA. The expression of RbAp48 in FRO cells stably transfected with siRNA plasmid (849) or control siRNA plasmid (1197) determined by Northern (A) and Western (B) blot. The RbAp48 mRNA expression levels were normalized on total RNA content, those of the RbAp48 protein on actin expression.

reason for such an interest is the possibility to interfere specifically with specific NF-κB effectors in transformed cells, without affecting other physiological cell functions regulated by NF-κB. We have developed a NF-κB null thyroid anaplastic cell line, by stably transfecting a superrepressor form of IκBα in the human anaplastic thyroid cell line FRO (FRO IκBαM) (20). We used this clone and its untransfected counterpart in a differential proteomic approach to identify gene products differentially expressed in the absence of functional NF-κB. RbAp48 was one of the proteins whose expression was down-regulated in the absence of functional NF-κB. The observed reduction was not due to a decreased stability of the protein, given that also the RbAp48 mRNA was decreased in FRO IκBαM clones, suggesting a direct control of NF-κB on RbAp48 expression. Two additional experimental evidences supported a role for NF-κB in the transcriptional control of RbAp48: 1) MEF isolated from the $p65^{-/-}$ mouse showed decreased levels of RbAp48 both mRNA and protein, and 2) the presence of a κB site in the promoter region of RbAp48. This κB site was functional, given that its deletion or mutation decreased the activity of the reporter plasmid induced by the NF-κB activator TNF-α by almost 50%. This also suggests that in addition to NF-κB, other transcription factors are controlling RbAp48 expression.

We also showed that RbAp48 expression was elevated in primary human thyroid carcinomas and correlated with the malignant phenotype. In particular, specimens as well as cell lines derived from anaplastic thyroid carcinomas showed the highest levels of RbAp48 expression (Table 1 and Fig. 3; data not shown). The pattern of RbAp48 expression in thyroid tumors parallels the levels of constitutive NF-κB activation we found in the same type of carcinomas (20), further supporting the idea that RbAp48 could be a NF-κB target gene.

Very little is known about the role of RbAp48 in cancer. Its expression has been found elevated in different human tumors, such as lung (30) and liver (31) cancer, acute myelocytic leukemia, and acute lymphoblastic leukemia (32). However, the mechanisms by which RbAp48 gene product could regulate tumor growth are largely unknown. We presented evidence that RbAp48 plays a role in thyroid cancer. Decreasing the expression of RbAp48 in FRO cells using siRNA abolished the ability of FRO cells to form colonies in soft agar. This effect was very likely due to a decrease of cell growth rate, which is one of the functions controlled by NF-κB during tumorigenesis (6). It is known that alteration of growth control is one of the features that, together with the dysregulation of other cell functions (apoptosis, angiogenesis, tissue invasion, *etc.*), could predispose to the genesis of cancer (33). The involvement of RbAp48 in cell growth control is not surprising because it has been shown that the double knockdown of RbAp48 and its homolog RbAp46, by RNA interference, leads HeLa cells to stop their growth, while the single ablation of either protein determines a slackening of cell proliferation (34). This is in accordance with

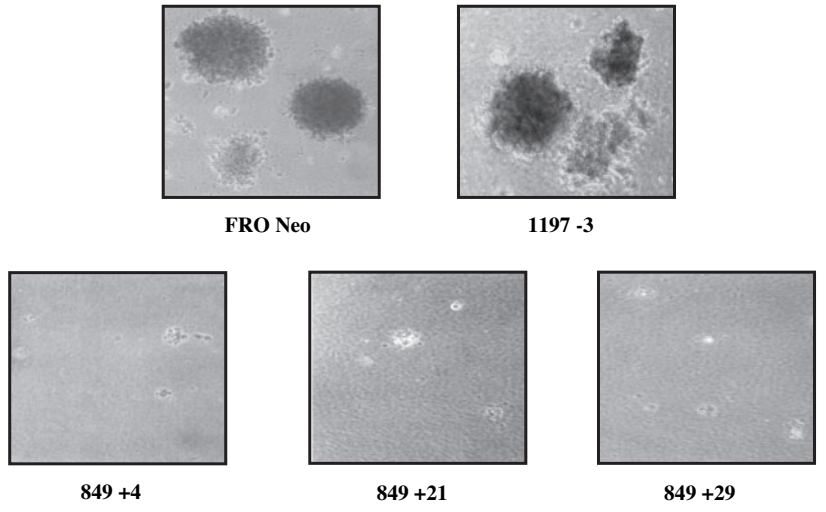

FIG. 5. *In vitro* oncogenic activity of FRO Neo cells and FRO siRNA clones. There were 1×10^4 cells seeded in 60-mm dishes onto 0.3% Noble Agar (Difco) on top of a 0.6% bottom layer. Colonies larger than 50 cells were scored after 2-wk incubation at 37 C. FRO Neo cells = >50 colonies/plate; 1197-3 cells = >40 colonies/plate; 849 + 4, +21, and +29 cells = 0 colonies/plate. Magnification, ×200.

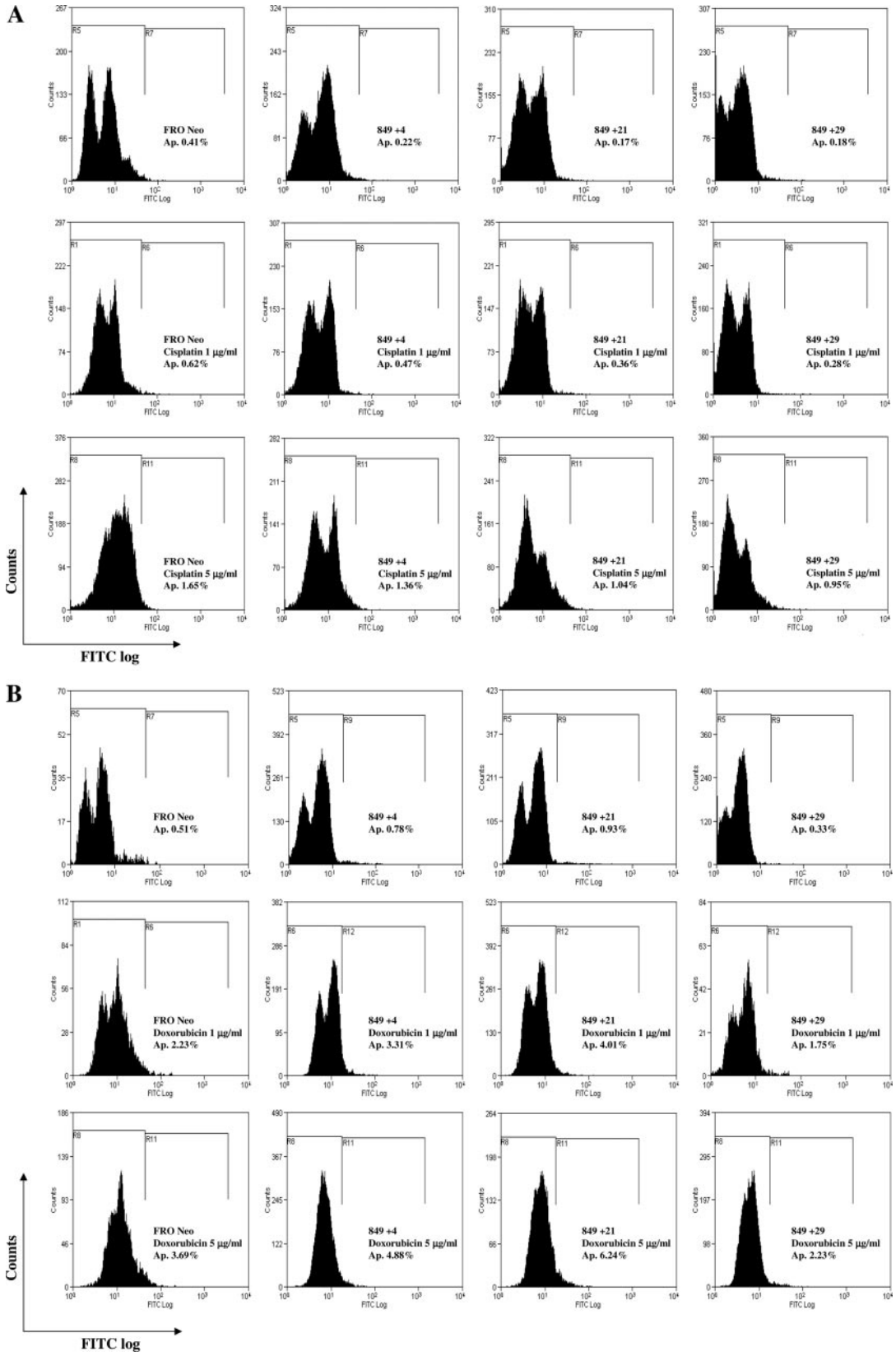

FIG. 6. Cytotoxic effects of chemotherapeutic drugs on FRO Neo cells and FRO siRNA clones. There were 2.5×10^5 cells/well seeded in six-well culture plates and incubated for 24 and 48 h at 37 C with different concentrations of cisplatin (A) or doxorubicin (B). Measuring caspase activity by the CaspACE FITC-VAD-FMK In Situ Marker (Promega) according to the manufacturer's instructions, assessed cell death. Samples were analyzed by flow cytometry using a CyAn ADP (DakoCytomation), equipped with Summit V4.2 Software. Results were mean ± SD of at least three separate experiments.

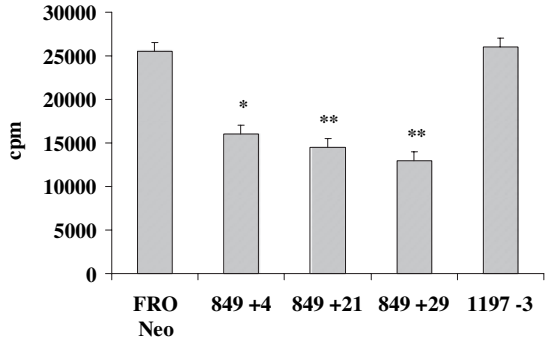

FIG. 7. Analysis of proliferative rate in FRO Neo cells and FRO siRNA clones. There were 5×10^4 cells/well seeded in 12-well culture plates and incubated for 4 h at 37 C with 0.5 μCi/well of [^{3}H]-thymidine (Amersham). After three washings with cold PBS, cells were incubated with 0.5 ml 20% trichloroacetic acid for 10 min at 4 C and then lysed. An aliquot of lysates was used to evaluate the protein content by colorimetric assay (Bio-Rad), whereas the remnant was analyzed at the β-counter (Beckman Coulter, Inc.). Results were the mean ± SD of two separate experiments. Significantly different from controls: *, $P < 0.05$; **, $P < 0.005$. Results were normalized on total protein content.

our data showing a decrease, but not a total block of growth rate, very likely because we knocked down only RbAp48, while RbAp46 was still able to overcome partially the functions of RbAp48.

Recently, numerous studies showed the use of HDAC inhibitors for the treatment of different thyroid cancer cell lines (35, 36). These molecules, including suberoylanilide hydroxamic acid, valproic acid, and others, potently suppress proliferation and induce apoptosis. RbAp48 has been characterized as a component of distinct nucleosome-modifying complexes, including HDAC, so it is tempting to speculate that the effect we observed on cell proliferation was dependent on the inhibition of HDAC activity in absence of RbAp48. However, we did not detect variation in HDAC activity in knock-down clones compared with the wild-type counterpart, nor difference in drug-induced apoptosis, suggesting that the observed effect on cell proliferation was not dependent on HDAC activity (Fig. 5; data not shown). Presently, we cannot exclude the possibility that the interference with cell proliferation is not the only mechanism by which RbAp48 contributes to thyroid tumorigenesis.

In summary, we identified RbAp48 as a NF-κB effector involved in thyroid cancer and showed that interfering with its expression decreases the autonomous growth of anaplastic thyroid carcinoma cells. Even so, further analysis is necessary to define better the molecular mechanisms by which RbAp48 acts in thyroid oncogenesis and whether it could represent a novel target for therapeutic intervention in NF-κB-dependent thyroid carcinomas.

Acknowledgments

The authors thank G. Salvatore for critical reading of the manuscript.

Received October 10, 2006. Accepted January 11, 2007.

Address all correspondence and requests for reprints to: Antonio Leonardi, Dipartimento di Biologia e Patologia Cellulare e Molecolare, Federico II University of Naples, Via S. Pansini 5, 80131 Naples, Italy. E-mail: leonardi@unina.it.

This work was supported by Associazione Italiana Ricerca sul Cancro.

Disclosure Statement: The authors have nothing to declare.

References

1. **Ghosh S, May MJ, Kopp EB** 1998 NF-κB and Rel proteins: evolutionarily conserved mediators of immune responses. Annu Rev Immunol 16:225–260
2. **Karin M, Ben-Neriah Y** 2000 Phosphorylation meets ubiquitination: the control of NF-κB activity. Annu Rev Immunol 18:621–663
3. **Tak PP, Firestein GS** 2001 NF-κB: a key role in inflammatory diseases. J Clin Invest 107:7–11
4. **Karin M** 1999 How NF-κB is activated: the role of the IκB kinase (IKK) complex. Oncogene 18:6867–6874
5. **Pahl HL** 1999 Activators and target genes of Rel/NF-κB transcription factors. Oncogene 18:6853–6866
6. **Karin M, Cao Y, Greten FR, Li ZW** 2002 NF-κB in cancer: from innocent bystander to major culprit. Nat Rev Cancer 2:301–310
7. **Greten FR, Eckmann L, Greten FT, Park JM, Li ZW, Egan LJ, Kagnoff MF, Karin M** 2004 IKKβ links inflammation and tumorigenesis in a mouse model of colitis-associated cancer. Cell 118:285–296
8. **Pikarsky E, Porat RM, Stein I, Abramovitch R, Amit S, Kasem S, Gutkovich-Pyest E, Urieli-Shoval S, Galun E, Ben-Neriah Y** 2004 NF-κB functions as a tumour promoter in inflammation-associated cancer. Nature 431:461–466
9. **Greten FR, Karin M** 2004 The IKK/NF-κB activation pathway-a target for prevention and treatment of cancer. Cancer Lett 206:193–199
10. **Kim HJ, Hawke N, Baldwin AS** 2006 NF-κB and IKK as therapeutic targets in cancer. Cell Death Differ 13:738–747
11. **Qian YW, Wang YC, Hollingsworth Jr RE, Jones D, Ling N, Lee EY** 1993 A retinoblastoma-binding protein related to a negative regulator of Ras in yeast. Nature 364:648–652
12. **Zhang Y, Ng HH, Erdjument-Bromage H, Tempst P, Bird A, Reinberg D** 1999 Analysis of the NuRD subunits reveals a histone deacetylase core complex and a connection with DNA methylation. Genes Dev 13:1924–1935
13. **Parthun MR, Widom J, Gottschling DE** 1996 The major cytoplasmic histone acetyltransferase in yeast: links to chromatin replication and histone metabolism. Cell 87:85–94
14. **Loyola A, Almouzni G** 2004 Histone chaperones, a supporting role in the limelight. Biochim Biophys Acta 1677:3–11
15. **Pazin MJ, Kadonaga JT** 1997 What's up and down with histone deacetylation and transcription? Cell 89:325–328
16. **Nicolas E, Morales V, Magnaghi-Jaulin L, Harel-Bellan A, Richard-Foy H, Trouche D** 2000 RbAp48 belongs to the histone deacetylase complex that associates with the retinoblastoma protein. J Biol Chem 275:9797–9804
17. **Nicolas E, Ait-Si-Ali S, Trouche D** 2001 The histone deacetylase HDAC3 targets RbAp48 to the retinoblastoma protein. Nucleic Acids Res 29:3131–3136
18. **Taylor-Harding B, Binnè UK, Korenjak M, Brehm A, Dyson NJ** 2004 p55, the Drosophila ortholog of RbAp46/RbAp48, is required for the repression of dE2F2/RBF-regulated genes. Mol Cell Biol 24:9124–9136
19. **Fagin JA, Matsuo K, Karmakar A, Chen DL, Tang SH, Koeffler HP** 1993 High prevalence of mutations of the p53 gene in poorly differentiated human thyroid carcinomas. J Clin Invest 91:179–184
20. **Pacifico F, Mauro C, Barone C, Crescenzi E, Mellone S, Monaco M, Chiappetta G, Terrazzano G, Liguoro D, Vito P, Consiglio E, Formisano S, Leonardi A** 2004 Oncogenic and anti-apoptotic activity of NF-κB in human thyroid carcinomas. J Biol Chem 279:54610–54619
21. **De Smaele E, Zazzeroni F, Papa S, Nguyen DU, Jin R, Jones J, Cong R, Franzoso G** 2001 Induction of gadd45β by NF-κB downregulates pro-apoptotic JNK signalling. Nature 414:308–313
22. **Thiede B, Dimmler C, Siejak F, Rudel T** 2001 Predominant identification of RNA-binding proteins in Fas-induced apoptosis by proteome analysis. J Biol Chem 276:26044–26050
23. **Salzano AM, Paron I, Pines A, Bachi A, Talamo F, Bivi N, Vascotto C, Damante G, Quadrifoglio F, Scaloni A, Tell G** 2006 Differential proteomic analysis of nuclear extracts from thyroid cell lines. J Chromatogr B Analyt Technol Biomed Life Sci 833:41–50
24. **Shevchenko A, Wilm M, Vorm O, Mann M** 1996 Mass spectrometric sequencing of proteins silver-stained polyacrylamide gels. Anal Chem 68:850–858
25. **Vascotto C, Cesaratto L, D'Ambrosio C, Scaloni A, Avellini C, Paron I, Baccarani U, Adani GL, Tiribelli C, Quadrifoglio F, Tell G** 2006 Proteomic analysis of liver tissues subjected to early ischemia/reperfusion injury during human orthotopic liver transplantation. Proteomics 6:3455–3465
26. **Zhang W, Chait BT** 2000 ProFound: an expert system for protein identification using mass spectrometric peptide mapping information. Anal Chem 72:2482–2489
27. **Mauro C, Pacifico F, Lavorgna A, Mellone S, Iannetti A, Acquaviva R, Formisano S, Vito P, Leonardi A** 2006 ABIN-1 binds to NEMO/IKKγ and co-operates with A20 in inhibiting NF-κB. J Biol Chem 281:18482–18488
28. **Maniatis T, Fritsch E, Sambrook J** 1989 Molecular cloning: a laboratory manual. Cold Spring Harbor, NY: Cold Spring Harbor Laboratory

29. **Macpherson I, Montagnier I** 1964 Agar suspension culture for the selective assay of cells transformed by polyoma virus. Virology 23:291–294
30. **Fukuoka J, Fujii T, Shih JH, Dracheva T, Meerzaman D, Player A, Hong K, Settnek S, Gupta A, Buetow K, Hewitt S, Travis WD, Jen J** 2004 Chromatin remodeling factors and BRM/BRG1 expression as prognostic indicators in non-small cell lung cancer. Clin Cancer Res 10:4314–4324
31. **Song H, Xia SL, Liao C, Li YL, Wang YF, Li TP, Zhao MJ** 2003 Genes encoding Pir51, Beclin 1, RbAp48 and aldolase b are up or down-regulated in human primary hepatocellular carcinoma. World J Gastroenterol 10:509–513
32. **Casas S, Ollila J, Aventin A, Vihinen M, Sierra J, Knuutila S** 2003 Changes in apoptosis-related pathways in acute myelocytic leukemia. Cancer Genet Cytogenet 146:89–101
33. **Hanahan D, Weinberg RA** 2000 The hallmarks of cancer. Cell 100:57–70
34. **Hayashi T, Fujita Y, Iwasaki O, Adachi Y, Takahashi K, Yanagida M** 2004 Mis16 and Mis18 are required for CENP-A loading and histone deacetylation at centromeres. Cell 118:715–729
35. **Mitsiades CS, Poulaki V, McMullan C, Negri J, Fanourakis G, Goudopoulou A, Richon VM, Marks PA, Mitsiades N** 2005 Novel histone deacetylase inhibitors in the treatment of thyroid cancer. Clin Cancer Res 11:3958–3965
36. **Catalano MG, Fortunati N, Pugliese M, Poli R, Bosco O, Mastrocola R, Aragno M, Boccuzzi G** 2006 Valproic acid, a histone deacetylase inhibitor, enhances sensitivity to doxorubicin in anaplastic thyroid cancer cells. J Endocrinol 191:465–472

JCEM is published monthly by The Endocrine Society (http://www.endo-society.org), the foremost professional society serving the endocrine community.